

## Article

# Chemical, Thermal, and Mechanical Properties of Sulfur Polymer Composites Comprising Low-Value Fats and Pozzolan Additives

Claudia V. Lopez <sup>1</sup>, Katelyn M. Derr <sup>1</sup>, Ashlyn D. Smith <sup>1</sup>, Andrew G. Tennyson <sup>1,2,\*</sup> and Rhett C. Smith <sup>1,\*</sup> 

<sup>1</sup> Center for Optical Materials Science and Engineering Technology, Department of Chemistry, Clemson University, Clemson, SC 29634, USA; cvlopez@g.clemson.edu (C.V.L.); klinden@g.clemson.edu (K.M.D.)

<sup>2</sup> Department Materials Science and Engineering, Clemson University, Clemson, SC 29634, USA

\* Correspondence: atennys@clemson.edu (A.G.T.); rhett@clemson.edu (R.C.S.)

**Abstract:** High sulfur-content materials (HSMs) formed via inverse vulcanization of elemental sulfur with animal fats and/or plant oils can exhibit remarkable mechanical strength and chemical resistance, sometimes superior to commercial building products. Adding pozzolan fine materials—fly ash (FA), silica fume (SF), ground granulated blast furnace slag (GGBFS), or metakaolin (MK)—can further improve HSM mechanical properties and stability. Herein, we detail nine materials comprised of rancidified chicken fat, elemental sulfur, and canola or sunflower oil (to yield CFS or GFS, respectively) and, with or without FA, SF, GGBFS, or MK. The base HSMs, CFS<sub>90</sub> or GFS<sub>90</sub>, contained 90 wt% sulfur, 5 wt% chicken fat, and 5 wt% canola or sunflower oil, respectively. For each HSM/fine combination, the resulting material was prepared using a 95:5 mass input ratio of HSM/fine. No material exhibited water uptake >0.2 wt% after immersion in water for 24 h, significantly lower than the 28 wt% observed with ordinary Portland cement (OPC). Impressively, CFS<sub>90</sub>, GFS<sub>90</sub>, and all HSM/fine combinations exhibited compressive strength values 15% to 55% greater than OPC. After immersion in 0.5 M H<sub>2</sub>SO<sub>4</sub>, CFS<sub>90</sub>, GFS<sub>90</sub>, and its derivatives retained 90% to 171% of the initial strength of OPC, whereas OPC disintegrated under these conditions. CFS<sub>90</sub>, GFS<sub>90</sub>, and its derivatives collectively show promise as sustainable materials and materials with superior performance versus concrete.

**Keywords:** sustainable polymer; sustainable composite; plant oil; animal fat; triglycerides; sulfur; sulfur cement; polymer cement



**Citation:** Lopez, C.V.; Derr, K.M.; Smith, A.D.; Tennyson, A.G.; Smith, R.C. Chemical, Thermal, and Mechanical Properties of Sulfur Polymer Composites Comprising Low-Value Fats and Pozzolan Additives. *Chemistry* **2023**, *5*, 2166–2181. <https://doi.org/10.3390/chemistry5040146>

Academic Editors: Bartolo Gabriele, José Antonio Odriozola and Edwin Charles Constable

Received: 11 September 2023

Revised: 9 October 2023

Accepted: 11 October 2023

Published: 12 October 2023



**Copyright:** © 2023 by the authors. Licensee MDPI, Basel, Switzerland. This article is an open access article distributed under the terms and conditions of the Creative Commons Attribution (CC BY) license (<https://creativecommons.org/licenses/by/4.0/>).

## 1. Introduction

Sustainable materials must achieve comparable performance to conventional materials as a prerequisite to widespread adoption and utilization [1,2]. Without comparable performance, sustainable materials will not be used to replace conventional materials despite their sustainability benefits. Concrete, for example, has a sizable carbon footprint, with roughly 1 ton of CO<sub>2</sub> being released into the atmosphere for each ton of concrete produced, [3–7] substantially worse than wood, whose carbon content of 434 kg per ton is equivalent to 1.59 tons of CO<sub>2</sub> being sequestered from the atmosphere per ton of wood used in a construction context [8,9]. However, concrete can be shaped more easily than wood and into a wider variety of forms, and it also exhibits superior resistance to environmental degradation, thus resulting in concrete being more widely used in structurally demanding construction applications. To be a viable alternative to concrete, a sustainable material must achieve concrete-like performance.

It is possible to increase the sustainability of an otherwise unsustainable construction material by modifying its composition. Sustainability improvements are not limited to the inclusion of biologically produced materials [10,11] but can also be achieved by including

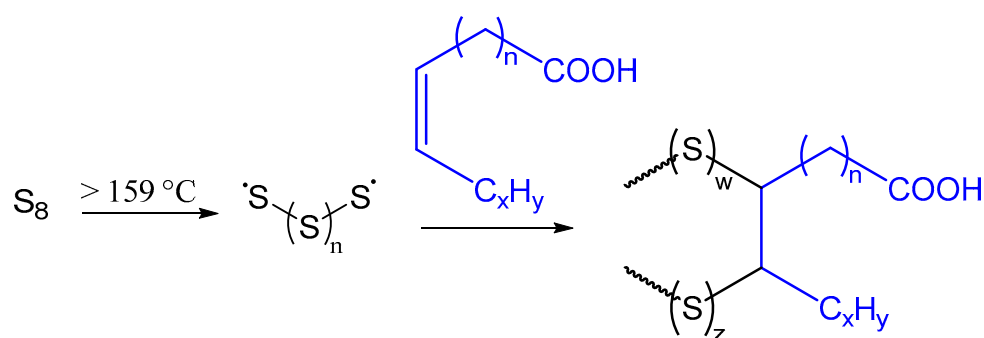
materials that would otherwise be discarded as waste and contribute to additional environmental hazards. An example of this is ground-granulated blast furnace slag (GGBFS), a by-product of iron smelting, a decidedly not environmentally friendly process. The incorporation of GGBFS into concrete as a substitute for other concrete components will, however, positively impact a material's rating in the LEED (Leadership in Energy and Environmental Design, from the U.S. Green Building Council) and BEAM (Building Environmental Assessment Method Plus, developed by the Hong Kong Green Building Council) rating systems for sustainability [12]. Therefore, one strategy we have employed for the development of sustainable alternatives to concrete has been to combine low-value co-products and/or waste products from other industrial processes into high-value materials that perform comparably or superior to conventional concretes [13–15].

Elemental sulfur, which exists primarily in the form of *cyclo-S<sub>8</sub>* under ambient conditions, [16,17] is a low-value co-product of petroleum refining, produced by hydrodesulfurization (HDS) processes developed to remove sulfur atoms from petrochemicals to prevent catalyst poisoning in subsequent refining steps and to reduce acid rain caused by the combustion of high-sulfur-content fuels. A staggering amount of elemental sulfur produced by HDS, >70 million metric tons, is produced annually via these processes, and unutilized sulfur is transported to solid waste storage sites [18–22].

For comparison, the US produced 95 million metric tons of cement in 2022; thus, in terms of sheer mass, elemental sulfur is an attractive alternative to cement and has been the subject of intense interest. High-sulfur-content materials (HSMs)—i.e., materials that contain >50 wt% of elemental sulfur—have already been shown to exhibit remarkable strengths that exceed that of load-bearing construction materials like OPC.

Replacing OPC with materials made from elemental sulfur would also have a tremendous impact on sustainability. The heavy carbon footprint of concretes derives primarily from OPC, whose production releases CO<sub>2</sub> both directly from the thermal decomposition of carbonate salts and indirectly from the energy required to heat these carbonates to temperatures >1200 °C. In fact, OPC production contributes approximately 8–10% of the total annual anthropogenic CO<sub>2</sub> greenhouse gas emissions [3]. Reaction temperatures for preparing HSMs range from 160 °C to 200 °C, corresponding to >80% less energy than required to heat OPC. Consequently, HSMs are significantly more sustainable than OPC-derived materials because they generate less atmospheric CO<sub>2</sub> and consume an otherwise unusable material discarded in waste storage sites, though they contain elemental sulfur produced by petroleum refining.

Inverse vulcanization is the process by which most HSMs are prepared from elemental sulfur [23,24]. Unlike traditional vulcanization, which strengthens natural rubber with small amounts of sulfur, inverse vulcanization utilizes sulfur as the main component and endows strength through the inclusion of small amounts of organics. Heating elemental sulfur to temperatures >159 °C induces ring-opening of *cyclo-S<sub>8</sub>* and subsequent formation of polymeric sulfur chains with radical termini (Scheme 1). Inverse vulcanization is performed in the presence of unsaturated organic molecules, whereby sulfur-centered radicals react with C=C bonds to yield crosslinked polymers or networked materials, depending on the structure of the organic species. This reactivity can achieve high degrees of crosslinking, which endows the resulting HSMs with strength profiles comparable to mineral-based materials. Another advantage of inverse vulcanization is its simplicity and atom-efficient nature. Furthermore, the ability of S–S  $\sigma$ -bonds in HSMs to undergo reversible bond-scission/reformation at relatively mild temperatures enables thermal recycling of many HSMs without deterioration in mechanical properties [25]. Beyond structural materials, HSMs prepared by inverse vulcanization have been used in a wide variety of applications, including lithium–sulfur batteries [26–30], infrared imaging [31], water purification [32–37], adhesives [38,39], and fertilizers [40–42].



**Scheme 1.** Inverse vulcanization examples wherein the unsaturated units of fatty acid substituents undergo a reaction with thermally-generated sulfur radical species.

The unsaturated organic species used as the co-reactant with *cyclo*-S<sub>8</sub> provides an additional avenue for enhancing material sustainability. Inverse vulcanization was pioneered by employing petroleum-derived alkenes in HSM syntheses [24,31,43–46], but any molecule with C=C bonds and sufficient miscibility in molten sulfur is mechanistically capable of undergoing an inverse vulcanization reaction to yield HSMs. A biologically produced unsaturated organic molecule contains carbon atoms that are all derived from atmospheric CO<sub>2</sub>. Even animal fats are assembled from smaller components and energy that can be traced back through the food chain to CO<sub>2</sub> absorbed by plants. Examples of biologically derived unsaturated organic molecules that can yield HSMs include fatty acids [47–49] and triglycerides [21,50–54].

Our group, in particular, has worked with a variety of biomass and plant-derived sources of olefins as chemical feedstocks for polymers and composites. We have even developed methodologies to prepare HSMs from biologically produced organics that would normally be incapable of undergoing inverse vulcanization via the functionalization of cellulose and lignin with olefin-bearing groups, for example. The HSMs prepared by our group using sustainable organics have achieved compressive strength, flexural strength, and chemical resistance superior to the values required of commercial OPC targeted for use in residential building foundations. Along this axis, we continue to explore various sources of biologically derived unsaturated organics.

Prior work in our group has shown that brown grease [55,56]—a mixture of oils and fats comprising >15% FFAs—can afford HSMs with structural properties that are competitive with commercial building materials [57,58]. However, the high viscosity of brown grease and its low miscibility with molten sulfur requires that brown grease be combined with plant oil prior to inverse vulcanization. We identified canola and sunflower oils as ideal additives to obtain brown grease-derived HSMs. Based on this precedence, we hypothesized that a 1:1 mixture of chicken fat, canola, or sunflower oil would undergo inverse vulcanization with elemental sulfur to yield an HSM that would serve both as a high-value structural material in its own right and as a binder for fine aggregates and pozzolans [59]—fly ash (FA), silica fume (SF), GGBFS, and metakaolin (MK)—yielding high-value concrete-like materials.

Chicken fat (CF) is a co-product of animal rendering processes. It has a high caloric content and is thus an attractive component for adding to animal feed. Unfortunately, some processes and degradation pathways lead to spoilage of fats via mechanisms such as triglyceride hydrolysis and oxidation. Because the presence of acid can catalyze triglyceride hydrolysis, the formation of free fatty acids (FFAs) from initial hydrolysis accelerates the hydrolysis and production of more FFAs. Triglyceride hydrolysis and oxidation yield products that give rise to the smell and taste of rancidity [60,61], whereby even 5% triglyceride hydrolysis can render a batch completely unusable for animal feed applications [62]. Once this has occurred, the rancidified animal fats must be disposed of as biohazardous wastes, and all energy and resources invested are lost. Given that the production of 1 kg of chicken

requires the consumption of 4300 L of water, it is imperative to find additional uses for rancidified chicken fat that is no longer suitable for use in foodstuffs [63].

Valorizing and productively employing rancid chicken fat, as well as brown grease, align well with the United Nations Sustainable Development Goals (SDGs) [64,65] covering aspects of responsible production and consumption (SDG 12), climate action (SDG 13), sustainable cities and communities (SDG 11), and innovative industrialization (SDG 9). By incorporating these wastes into high-value HSMs, rancid chicken fat, and brown grease further improve sustainability indices, enhance environmental consciousness, and harmonize enterprises with broader socio-environmental economic needs.

Herein, we report composites based on CFS<sub>90</sub> or GFS<sub>90</sub>, these HSMs comprising 5 wt% rancidified chicken fat, 5 wt% canola or sunflower oil, and 90 wt% elemental sulfur [66]. Specifically, we explore the impact of adding 10 wt% FA, SF, GGBFS, or MK to CFS<sub>90</sub> and GFS<sub>90</sub>. Impressively, CFS<sub>90</sub>, GFS<sub>90</sub>, and CFS<sub>90</sub>/GFS<sub>90</sub>-derived materials exhibited 15% to 55% greater compressive strengths than OPC, water uptake values  $\leq 0.2$  wt% (vs. 28 wt% for OPC), and superior resistance to acidic corrosion.

## 2. Materials and Methods

### 2.1. Chemical Precursor Sources

Elemental sulfur (99.5%, Alfa Aesar, Maverhill, MA, USA) was used without further purification. Fly ash (FA), silica fume (SF), and ground granulated blast furnace slag (GGBFS) pozzolanic cement components were purchased from Diversified Minerals, Inc. (Oxnard, CA, USA), while metakaolin was manufactured by Opptipozz and the fines were used without further purification. Rancidified chicken fat was obtained from an industrial supplier with an olefin content of  $2.7 \text{ mmol} \cdot \text{g}^{-1}$ .

CAUTION: Heating elemental sulfur with organics can result in the formation of H<sub>2</sub>S gas. H<sub>2</sub>S is toxic, foul-smelling, and corrosive [67–69].

### 2.2. Thermal Analysis

TGA data were recorded (Mettler Toledo TGA 2 STARe System) over the range of 20–800 °C with a heating rate of  $10 \text{ }^\circ\text{C} \cdot \text{min}^{-1}$  under a flow of N<sub>2</sub> ( $100 \text{ mL} \cdot \text{min}^{-1}$ ). Each measurement was acquired in duplicate, and the presented results represent an average value.

### 2.3. Synthesis of CFS<sub>90</sub>

This procedure follows the reported method [58,66]. Elemental sulfur (180.0 g, 90 wt%) was added to a 500 mL Erlenmeyer flask. The vessel was placed in a thermostat-controlled oil bath set to 180 °C and stirred with an overhead mechanical stirrer equipped with a stainless steel stir rod and vane. Elemental sulfur was initially heated at 160 °C. Upon further heating, the viscosity of elemental sulfur increased, and a deep red color characteristic of polymeric sulfur radicals was noticed. Once the temperature was stable, the chicken fat (10.0 g, 5 wt%) was slowly added to the sulfur while stirring. Then, canola oil (10.0 g, 5 wt%) was added dropwise to the mixture. The reaction mixture was stirred for 24 h at 185 °C. After cooling to room temperature, the materials were rigid brown to black solids that were readily re-meltable and could be shaped into compressive test cylinders by being poured into silicone molds.

### 2.4. Synthesis of GFS<sub>90</sub>

This procedure follows the reported method [58]. Elemental sulfur (180.0 g, 90 wt%) was added to a 500 mL Erlenmeyer flask. The vessel was placed in a thermostat-controlled oil bath set to 180 °C and stirred with an overhead mechanical stirrer equipped with a stainless steel stir rod and vane. Elemental sulfur was initially heated at 160 °C. Upon further heating, the viscosity of elemental sulfur increased, and a deep red color characteristic of polymeric sulfur radicals was noticed. Once the temperature was stable, the chicken fat (10.0 g, 5 wt%) was slowly added to the sulfur while stirring. Then, sunflower oil (10.0 g, 5 wt%) was added dropwise to the mixture. The reaction mixture was stirred for 24 h at

185 °C. After cooling to room temperature, the materials were rigid brown to black solids that were readily re-meltable and could be shaped into compressive test cylinders by being poured into silicone molds.

### 2.5. General Procedure for the Addition of Fines to Binders

CAUTION: Heating elemental sulfur with organics can result in the formation of H<sub>2</sub>S gas. H<sub>2</sub>S is toxic, foul-smelling, and corrosive.

This procedure follows a reported method for adding fines to fatty acid–sulfur cement [15]. The requisite binder, CFS<sub>90</sub> or GFS<sub>90</sub> (33.0 g, 90 wt%), was melted in a 125 mL Erlenmeyer flask equipped with a Teflon-coated magnetic stir bar. The flask was submerged in a thermostat-controlled oil bath set to 180 °C. Once the binder had fully melted, the corresponding pozzolan (3.7 g, 10 wt%) was added with rapid stirring. After rapid stirring for 1 h, the mixture was removed from the heat, and cylinders for compressional analysis were prepared by pouring the molten mixture into silicone cylinder molds. All mixtures could also be re-melted for shaping later as needed.

### 2.6. Compressional Measurements

Compressional measurements were acquired on cylinders (Figure 1) using a Mark-10 ES30 (Mark-10 Corporation, Copiague, NY, USA) Manual Test Stand equipped with a Mark 10 M3-200 Force Gauge (Mark-10 Corporation Copiague, NY, USA) by a modified ASTM C39 standard. All materials were allowed to stand at room temperature for 4 d prior to compressional strength testing. The four-day aging period was selected after assessing material properties over shorter and longer times for one set of samples, and the properties were leveled off after 4 d. Longer-term stability is not known for these materials.

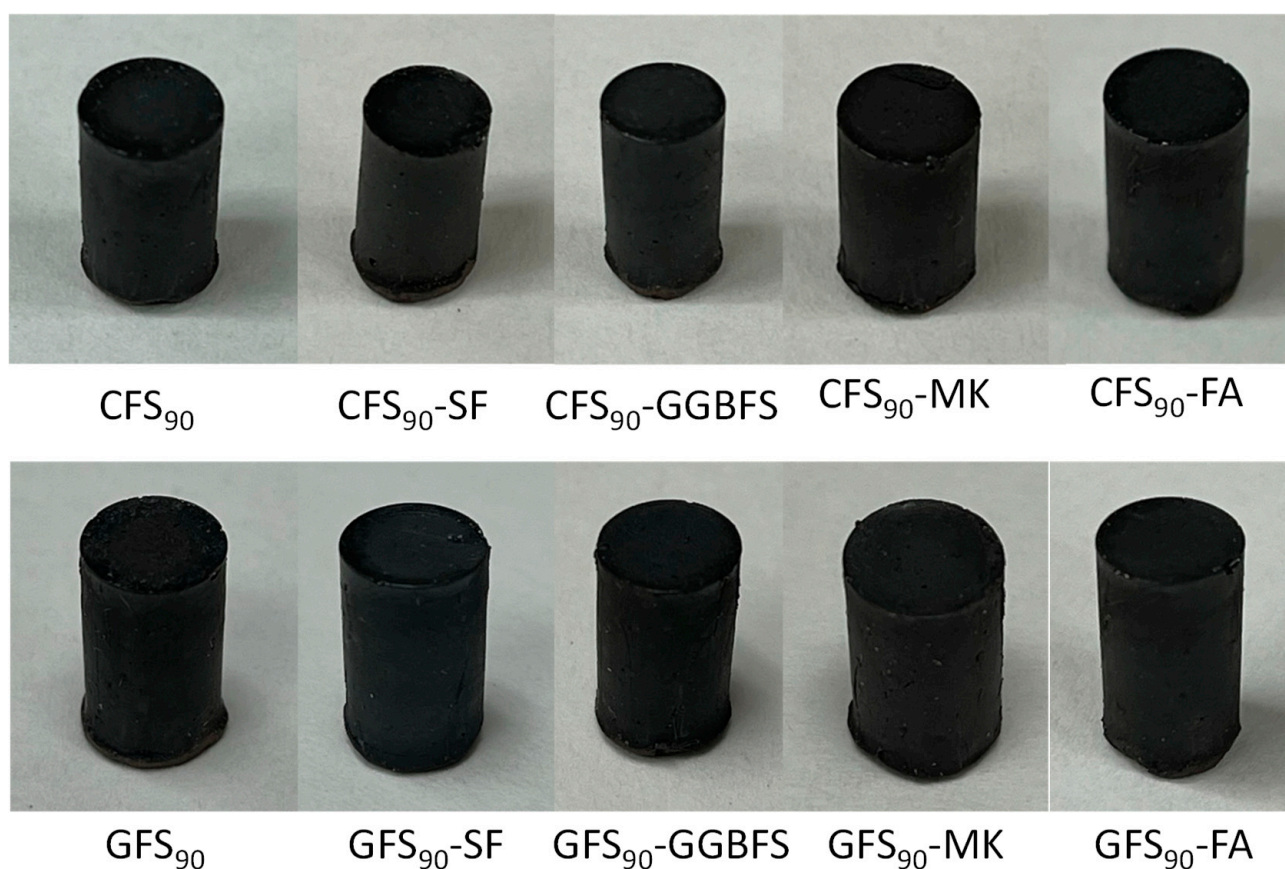


**Figure 1.** Samples of CFS<sub>90</sub>, CFS<sub>90</sub>-SF, CFS<sub>90</sub>-GGBFS, CFS<sub>90</sub>-MK, CFS<sub>90</sub>-FA, GFS<sub>90</sub>, GFS<sub>90</sub>-SF, GFS<sub>90</sub>-GGBFS, and GFS<sub>90</sub>-MK shaped for compressive testing.

### 3. Results

#### 3.1. Selection and Properties of Starting Materials

##### 3.1.1. Chicken Fat

As noted previously, rancidified chicken fat contains elevated levels of free fatty acids (FFAs) caused by triglyceride decomposition and is a major undesired by-product prevalent in animal rendering processes. Thus, there is an urgent need to develop productive uses for rancidified CF. Non-food uses for high-FFA chicken fat have been investigated, primarily focusing on soapmaking and biodiesel production [70,71]. Rancidified chicken fat used in this study contains C=C bonds at an abundance of  $2.70 \text{ mmol}\cdot\text{g}^{-1}$ , which provides the requisite chemical functionality to undergo inverse vulcanization with elemental sulfur.

##### 3.1.2. Fly Ash (FA)

Fly ash is a by-product of coal combustion consisting of fine particles collected and filtered in electrostatic precipitators [72]. Fly ash typically consists of spherical, glassy particles with an average diameter ranging from 0.5 to 100  $\mu\text{m}$ ; the chemical composition consists primarily of silicon-, aluminum-, and iron-oxides. In the cement industry, FFA has demonstrated success as a complementary additive to Portland cement, where the resulting cement blends exhibit enhanced material durability. Additionally, using FA decreases the adverse environmental impacts of construction activities by utilizing waste material and reducing the amount of OPC consumed. The fineness modulus of FA used in this study was 2.53. The fineness modulus is a dimensionless parameter used to categorize the uniformity of granular particles. It is a statistical mean from a sieve analysis using distinct standard sizes for sieving the aggregate, evaluating cumulative mass retained on each sieve, considering their sum, and normalizing that sum by a factor of 100. The fineness moduli of the pozzolan powders used herein were characterized as previously reported [15].

##### 3.1.3. Silica Fume (SF)

Silica fume, also known as microsilica, is composed of noncrystalline particles produced by the combustion of silicon and ferrosilicon alloys in high-temperature electric arc furnaces [73]. Chemically, SF primarily consists of amorphous  $\text{SiO}_2$ , with trace amounts of other oxides. Like FA, silica fume is a valuable supplement to cement by enhancing its mechanical properties, such as compressive strength. Overall, SF provides significant benefits in producing high-performance and sustainable cementitious materials. The fineness modulus of SF used in this study was 3.78.

##### 3.1.4. Ground-Granulated Blast Furnace Slag (GGBFS)

Ground-granulated blast furnace slag (GGBFS) is a by-product of the smelting of iron-containing ores in a blast furnace [74]. GGBFS produced in this manner is an amorphous, granular powder consisting primarily of calcium silicates and aluminosilicates similar to those found in OPC. The incorporation of GGBFS into OPC increases the compressive strength and durability of concrete and represents an effective resource and waste management technique that contributes to sustainable construction practices. The fineness modulus of GGBFS used in this study was 3.35.

##### 3.1.5. Metakaolin (MK)

Metakaolin is an amorphous, dehydroxylated form of kaolin [75]. Metakaolin predominantly consists of amorphous  $\text{SiO}_2$  and  $\text{Al}_2\text{O}_3$ , with trace amounts of other silicon- and aluminum oxides. When added to cement, MK enhances its strength and durability. The fineness modulus of MK used in this study was 4.63.

#### 3.2. Preparation of Polymer and Polymer-Fines Composites

Preparations of  $\text{CFS}_{90}$  and  $\text{GFS}_{90}$  were carried out as previously described for  $\text{SunBG}_{90}$ , an HSM made from the reaction of 90 wt% elemental sulfur, 5 wt% brown grease (olefin content  $3.24 \text{ mmol}\cdot\text{g}^{-1}$ ), and 5 wt% sunflower oil [58]. Fines-incorporating composites

containing CFS<sub>90</sub> or GFS<sub>90</sub> were prepared by remelting CFS<sub>90</sub> or GFS<sub>90</sub> at 180 °C and mixing it with 10 wt% of the desired fine aggregate, using rapid mechanical stirring to achieve homogeneity. After 1 h, these mixtures were liquids of brown or black color, giving brown to black, re-meltable solids when cooled to room temperature. Combining CFS<sub>90</sub> (Figure 1A) with 5 wt% FA, SF, GGBFS, or MK afforded the HSM/fine composites CFS<sub>90</sub>-FA, CFS<sub>90</sub>-SF, CFS<sub>90</sub>-GGBFS, and CFS<sub>90</sub>-MK, respectively (Figure 1). Similarly, combining GFS<sub>90</sub> (Figure 1) with FA, SF, GGBFS, and MK in this manner afforded the HSM/fine composites GFS<sub>90</sub>-FA, GFS<sub>90</sub>-SF, GFS<sub>90</sub>-GGBFS, and GFS<sub>90</sub>-MK, respectively (Figure 1). Consistent with prior work on brown grease-derived HSM/fine composites, all of the chicken fat-derived composites prepared in this work could be re-melted and recast into a variety of shapes such as the cylinders shown in Figure 1, with the exception of GBS<sub>90</sub>-FA, which, while re-meltable, was too viscous to practically shape using the usual method, so GBS<sub>90</sub>-FA was not further explored.

Scanning electron microscopy with elemental mapping using energy dispersive X-ray analysis (SEM-EDX) of CFS<sub>90</sub>-derived composites showed uniform distributions of carbon, oxygen, and sulfur in the HSM domains, with voids in the high-sulfur domains at particles of the added pozzolan fines (Figure 2), as expected for a composite in which the added particles have not been chemically disintegrated. These data are consistent with the other three reports in which these pozzolans were used as additives for HSMs [13–15].

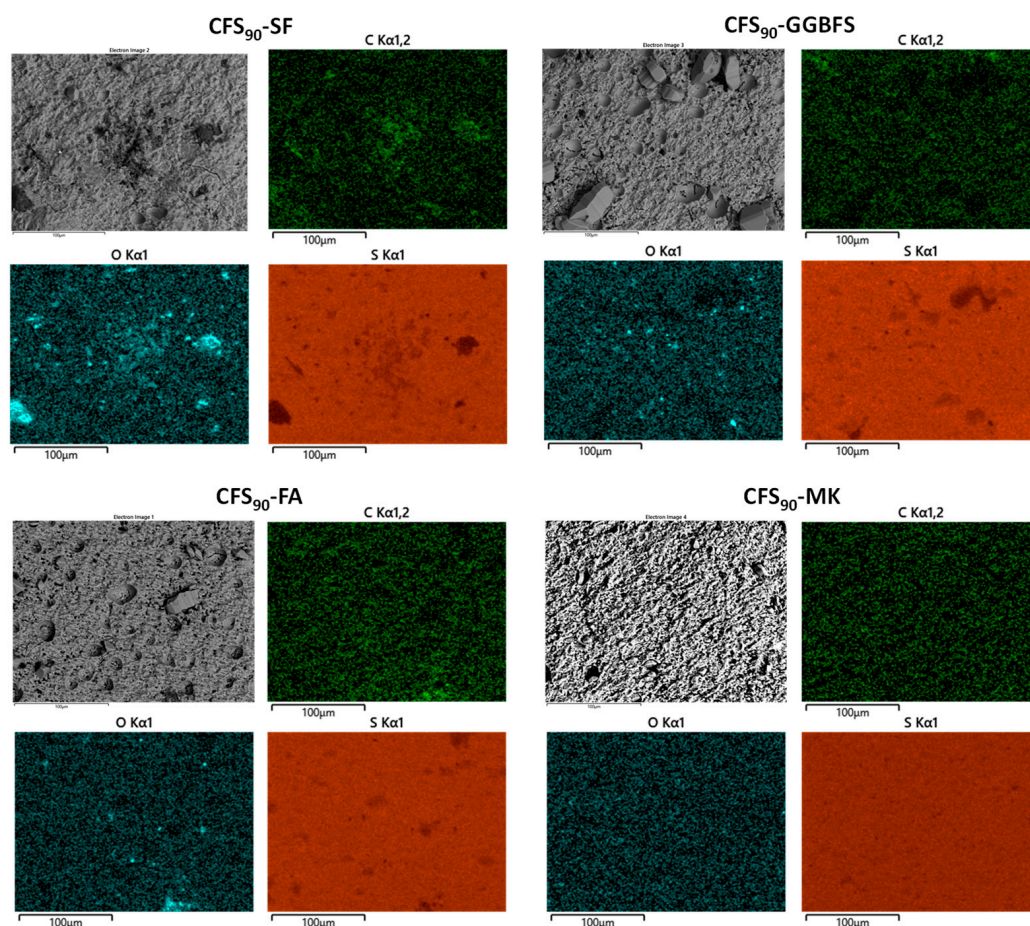


**Figure 2.** Surface analysis of the CFS<sub>90</sub>-derived composites using SEM (gray) with elemental mapping via EDX for sulfur (red), carbon (green), and oxygen (cyan). The scale bar in each image is 100 microns.

### 3.3. Thermal/Mechanical Properties and Acid Resistance

Water absorption into a material renders it more vulnerable to mechanical damage via freeze/thaw cycling; thus, the pursuit of water-repellent derivatives and alternatives to conventional cement can significantly extend its operational lifespan. Given the fact that CFS<sub>90</sub>/GFS<sub>90</sub> and its composites contain 90 wt% sulfur and that sulfur is hydrophobic, we envisioned that the parent HSM and its composites would exhibit water-repellent behavior. Water uptake by the parent HSM CFS<sub>90</sub>, GFS<sub>90</sub>, and the composites with FA, SF, GGBFS, and MK was therefore evaluated using the ASTM D570 standard test conditions in which each sample was completely submerged in water for 24 h at room temperature. The extent of water uptake was quantified as %H<sub>2</sub>O<sub>abs</sub> (Table 1). Calculated using this equation:

$$\%H_2O_{abs} = [(Wet\ weight - Dry\ weight)/Dry\ weight] \times 100$$

**Table 1.** Physical and mechanical properties of high sulfur content composites.

Material	Water Uptake (wt%)	Density (kg·m <sup>3</sup> )	Initial Compressive Strength (MPa)	Post-Acid Strength (MPa)	Retained Strength (% of Pre-Acid)
CFS <sub>90</sub>	0	1.700	24.7 ± 0.7	29.1 ± 2.5	120
CFS <sub>90</sub> -SF	0.2	1.700	25.8 ± 2.3	15.3 ± 1.8	59
CFS <sub>90</sub> -GGBFS	0	1.700	26.3 ± 1.4	24.4 ± 1.1	93
CFS <sub>90</sub> -MK	0	1.500	23.7 ± 2.1	18.4 ± 1.3	78
CFS <sub>90</sub> -FA	0.1	1.600	22.6 ± 1.1	25.1 ± 0.4	110
GFS <sub>90</sub>	0	1.700	24.9 ± 0.9	26.5 ± 0.8	110
GFS <sub>90</sub> -SF	0	1.700	24.3 ± 1.3	25.2 ± 1.4	100
GFS <sub>90</sub> -GGBFS	0.1	1.700	26.7 ± 0.2	26.6 ± 2.6	99
GFS <sub>90</sub> -MK	0.1	1.600	19.3 ± 0.5	19.1 ± 2.2	98
SunBG <sub>90</sub>	0.8	1.700	35.9 ± 0.7	NA	NA
OPC [76]	>28	1.500	17.0	0	0

Quantitatively zero water uptake was observed in the parent HSMs CFS<sub>90</sub>, GFS<sub>90</sub>, and the composites CFS<sub>90</sub>-FA and CFS<sub>90</sub>-GGBFS following complete submersion in water for 24 h. The values were exceedingly low (0.1–0.2 wt%) for CFS<sub>90</sub>-SF, CFS<sub>90</sub>-MK, GFS<sub>90</sub>-GGBFS, and GFS<sub>90</sub>-MK. Interestingly, CFS<sub>90</sub> and GFS<sub>90</sub> had superior water-repellency compared to its brown grease-derived analog, SunBG<sub>90</sub>, which exhibited a water uptake of 0.83 wt% [58]. For comparison, OPC exhibits water uptake values as high as 28 wt%, more than 100-fold higher than the HSM composites reported here.

Density values ( $\rho$ ) of CFS<sub>90</sub>, GFS<sub>90</sub>, and CFS<sub>90</sub>/GFS<sub>90</sub>-derived composites were measured for compressive strength test cylinders such as those shown in Figure 1 prior to conducting compressive strength tests. All materials prepared in this work exhibited density values ranging from 1.500 to 1.700 kg·m<sup>-3</sup>, comparable to OPC itself ( $\rho = 1.500$  kg·m<sup>-3</sup>) and in good agreement with the brown grease-derived HSM analog of CFS<sub>90</sub> or GFS<sub>90</sub> ( $\rho = 1.700$  kg·m<sup>-3</sup>). The values observed with CFS<sub>90</sub>, GFS<sub>90</sub>, and fines-derived composites demonstrate that these materials comply with the American Concrete Institute (ACI) standard ACI-213R and ASTM 169C density recommendations, thereby qualifying CFS<sub>90</sub>, GFS<sub>90</sub>, and all the fines-HSM derived composites as lightweight structural materials ( $\rho = 1.500$ – $1.800$  kg·m<sup>-3</sup>, Table 1).

Structural load-bearing materials must exhibit high compressive strength, which is one of the characteristic features of OPC and OPC-derived concretes. Whereas there has been significant work towards improving and understanding tensile properties of HSMs, [53,77,78] building regulations such as for cement that will be used in the foundations and/or footings of residential buildings must exhibit high compressive strength of  $\geq 17$  MPa (ACI specification 332.1R-06). With regards to this property, CFS<sub>90</sub> and CFS<sub>90</sub>-derived composites all easily met this threshold, ranging from  $22.6 \pm 1.1$  MPa for CFS<sub>90</sub>-FA at the low end to  $26.3 \pm 1.4$  MPa for CFS<sub>90</sub>-GGBFS at the high end, or 133% to 155% the

compressive strength of conventional OPC (Figure 3A; stress-strain plots are provide in Figures S1–S8 of the Supplementary Materials). Similarly, GFS<sub>90</sub> and GFS<sub>90</sub>-derived composites exhibited compressive strengths ranging from  $19.3 \pm 0.5$  MPa for GFS<sub>90</sub>-MK to  $26.7 \pm 0.2$  MPa for GFS<sub>90</sub>-GGBFS at the high end, which represents between 114 and 157% of the compressive strength of traditional OPC (Figure 3B). The compressive strength of CFS<sub>90</sub> and GFS<sub>90</sub> was notably lower than that of the analogous BG-based HSM, SunBG<sub>90</sub>, previously reported by our group ( $35.9 \pm 0.7$  MPa), which likely reflects the lower olefin content of chicken fat compared to brown grease used to prepare the HSMs ( $2.70 \text{ mmol}\cdot\text{g}^{-1}$  vs.  $3.24 \text{ mmol}\cdot\text{g}^{-1}$ , respectively). As the abundance of C=C bonds per unit mass in a material increases, that unit of mass can undergo greater reactions with elemental sulfur, thereby giving rise to a higher density of crosslinking polysulfide chains per unit mass of HSM. As the density of crosslinking chains in an HSM increases, the bulk material will more strongly resist deformation.

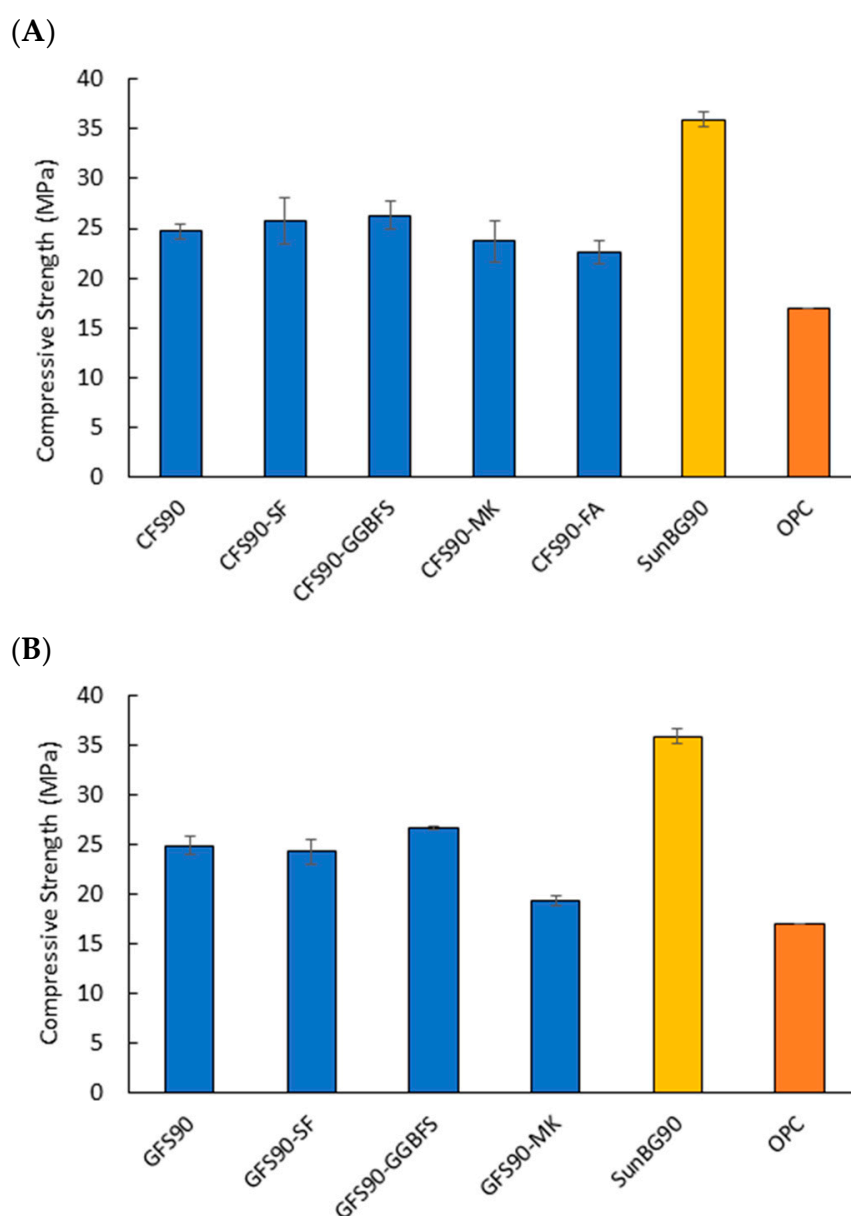


**Figure 3.** Comparison of compressive strengths of CFS<sub>90</sub>-derived composites (A) and GFS<sub>90</sub>-derived composites (B) to OPC and some other fat-incorporating HSMs.

Thermal and chemical stability are also important considerations when assessing the viability of binders to replace OPC. Thermogravimetric analysis (TGA) of binders CFS<sub>90</sub> and GFS<sub>90</sub> revealed decomposition temperatures of 224 °C and 218 °C, both well above the operational temperature expected for standard paving applications. Whereas the alkaline, ionic composition of OPC (e.g., CaO, Al<sub>2</sub>O<sub>3</sub>, etc.) causes it to react readily with Bronsted acids, the non-polar composition of CFS<sub>90</sub> and GFS<sub>90</sub> (i.e., sulfur and triglycerides) should strongly disfavor, if not eliminate entirely, Bronsted acid–base reactivity. To test for susceptibility to acid-induced damage, compressive strength test cylinders of CFS<sub>90</sub>, GFS<sub>90</sub>, and HSMs-fines derived composites were prepared and fully submerged in 0.5 M H<sub>2</sub>SO<sub>4</sub> for 24 h (Figure 4). After 24 h, the cylinders were isolated, rinsed with H<sub>2</sub>O, and patted dry, and then their compressive strengths were measured. When a cylinder of OPC was subjected to this acid challenge, complete disintegration was observed within the 24 h test period. Thus, the compressive strength of OPC after an acid challenge was 0% of the compressive strength of OPC before the acid challenge. In contrast, the compressive strengths of CFS<sub>90</sub> and CFS<sub>90</sub>-derived composites after the acid challenge were 90% to 171% that of OPC before the acid challenge (Figure 5A). Similarly, the compressive strength of GFS<sub>90</sub> and GFS<sub>90</sub>-derived composites after the acid challenge was between 114% and 156% that of OPC before the acid challenge (Figure 5B).

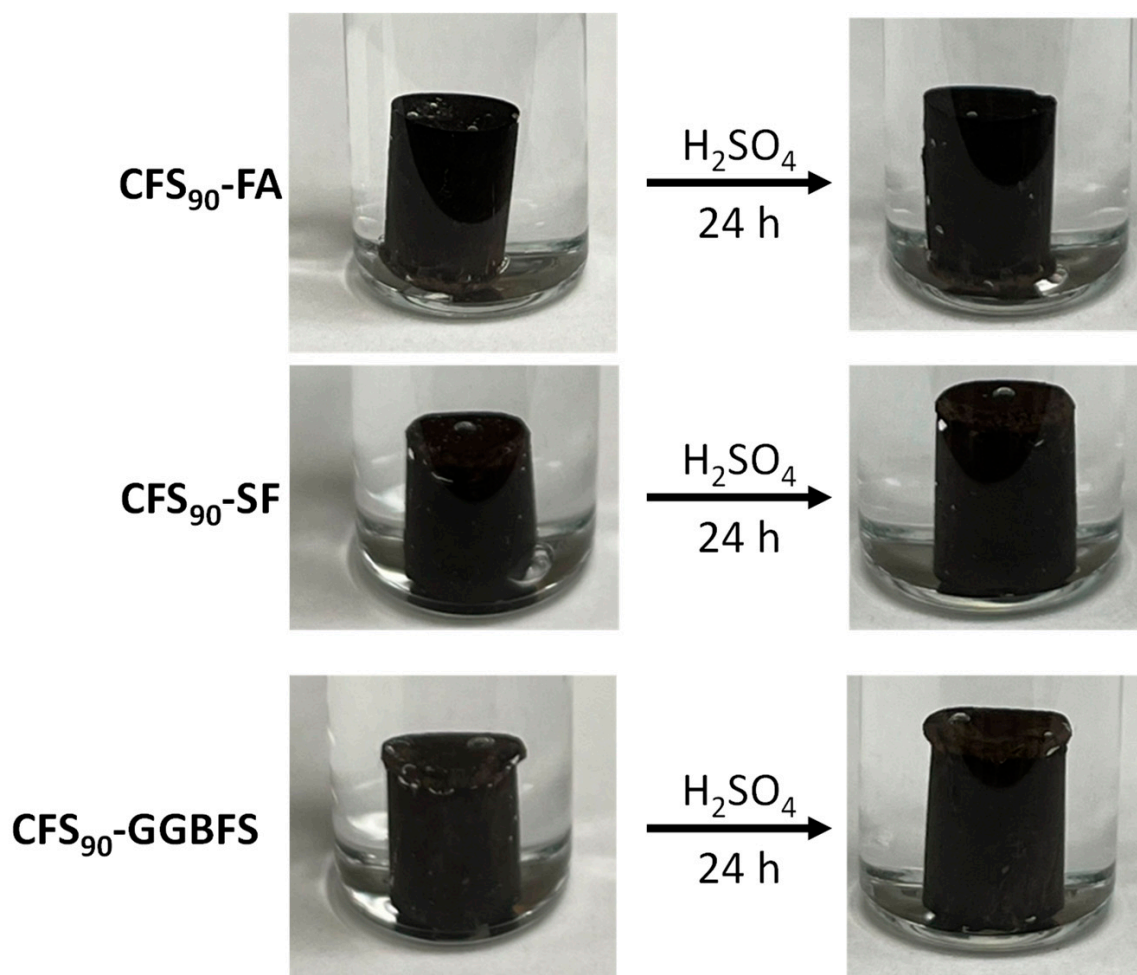


**Figure 4.** Representative samples of CFS<sub>90</sub>-FA, CFS<sub>90</sub>-SF, and GFS<sub>90</sub>-GGBFS, before (left) and after (right) being submerged in 0.5 M H<sub>2</sub>SO<sub>4</sub> for 24 h.

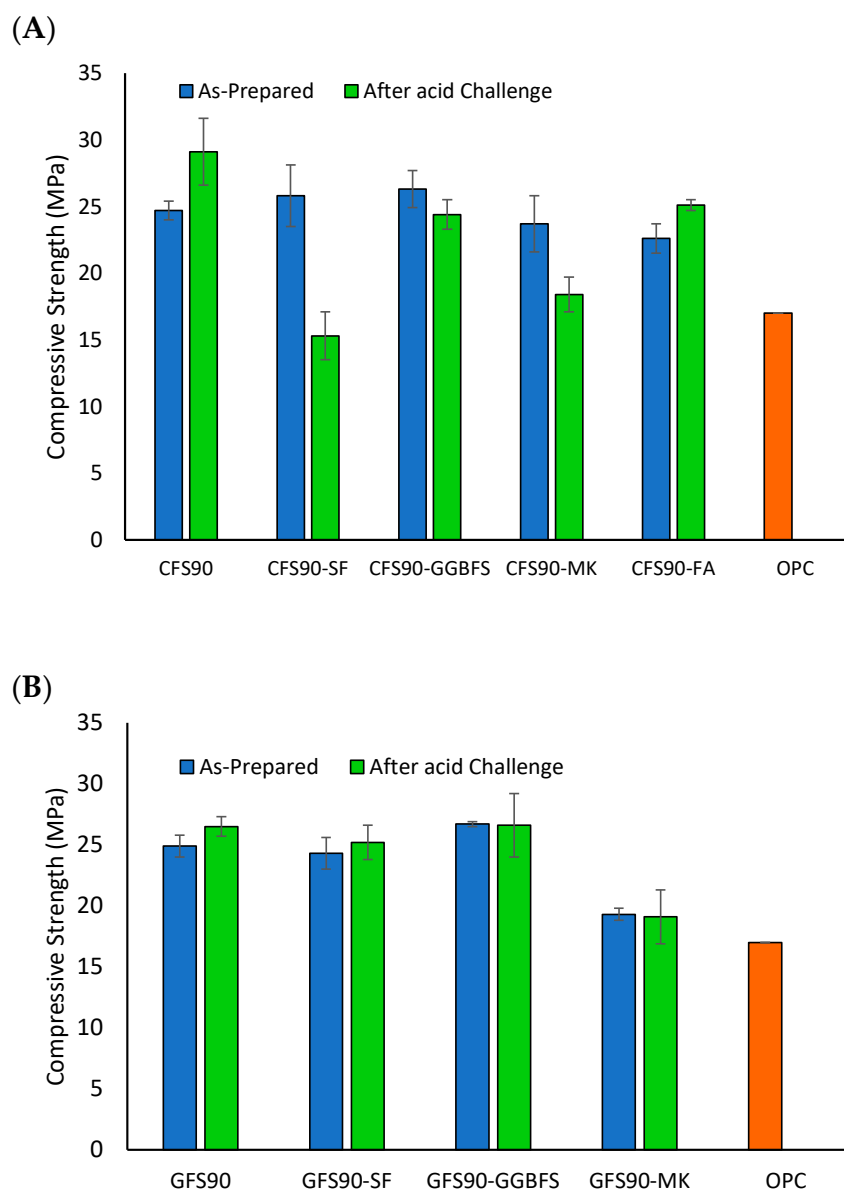


**Figure 5.** Comparison of compressive strengths of CFS<sub>90</sub>-derived (A) and GFS<sub>90</sub>-derived (B) composites before (blue-colored bars) and after (green-colored bars) exposure to 0.5 M H<sub>2</sub>SO<sub>4</sub> for 24 h. OPC is shown by the orange bar for comparison.

#### 4. Conclusions

Concrete production is one of the largest sources of atmospheric CO<sub>2</sub> and is thus a major contributor to climate change. Although the CO<sub>2</sub> indirectly generated by the electricity consumed in concrete production could, in principle, be eliminated using renewable energy sources, the CO<sub>2</sub> directly generated by the CaCO<sub>3</sub> → CaO + CO<sub>2</sub> reaction required for OPC could not be eliminated without finding a carbon-free alternative to OPC. In addition to its significant carbon footprint, concrete production consumes vast amounts of fresh water, simultaneously reducing the availability of safe drinking water for vulnerable populations across the world. Thus, achieving a truly sustainable and equitable economy is impossible without replacing OPC and OPC-derived concretes.

The composite structure of concrete, consisting of a binder (OPC) with fines and aggregate, offers multiple avenues for developing sustainable alternatives to concrete. Whereas the production of OPC releases CO<sub>2</sub> into the atmosphere, the formation of triglycerides in plants instead formally removes CO<sub>2</sub> from the atmosphere, and the carbon feedstocks

for animals are plants and/or other animals. Because the organics employed in this work were chicken fat and sunflower oil, the composites derived from these organics functionally sequester atmospheric CO<sub>2</sub>. As a result, the composites detailed in this work can serve as CO<sub>2</sub>-sequestering alternatives to CO<sub>2</sub>-emitting construction materials.

Elemental sulfur is a versatile monomer for binder synthesis, given that its S–S bonds reversibly undergo bond breakage/reformation under relatively mild thermal conditions, enabling the preparation of HSMs with a variety of polymeric sulfur chain lengths. This, in turn, enables the HSMs to be melted and cast into a variety of shapes and to be recycled thermally. The hydrophobic nature of elemental sulfur endows HSMs with excellent water repellency, preventing the uptake of water that is a prerequisite for multiple damage mechanisms (freeze/thaw, corrosion, etc.). The composites reported in this work exhibit minuscule water-uptake values of 0% to 0.2%. Furthermore, the gargantuan quantities of elemental sulfur sitting in waste storage sites, for which there are currently no valuable uses, make it an inexpensive, readily abundant feedstock material. Even if all petroleum refining ceased overnight, the tens of millions of tons of elemental sulfur produced over the decades would still be sitting in waste storage sites. Thus, not only do the HSMs reported in this work serve as CO<sub>2</sub>-sequestering construction material alternatives to OPC-based concretes, but they also convert low-value waste into high-value products.

The fines explored in this work (SF, MK, FA, and GGBFS) represent an additional vector for valorization and enhancing sustainability. Each of these fines is a relatively low-value by-product or co-product of other industrial processes, and they have all been used in OPC-based concretes. With GGBFS specifically, it has been reported to afford stronger OPC-based concretes compared to other fines and materials that increase in strength over time. Consistent with these findings, the composites exhibit compressive strength values 14% to 55% greater than that of OPC. Impressively, each composite can be immersed in 0.5 M H<sub>2</sub>SO<sub>4</sub> for 24 h and still exhibit compressive strength values of 90% to 160% of OPC. In contrast, acid-challenging OPC under these conditions leads to a total loss of mechanical strength.

Our findings demonstrate conclusively that CFS<sub>90</sub>, GFS<sub>90</sub>, and HSMs fines-derived composites exhibit vastly superior mechanical strength, water repellency, and corrosion resistance compared to OPC and OPC-based concretes. Furthermore, the organic components of CFS<sub>90</sub>, GFS<sub>90</sub>, and HSMs-fines composites are ultimately derived from atmospheric CO<sub>2</sub>, which allows them to simultaneously function as carbon-storage materials. With CFS<sub>90</sub>, GFS<sub>90</sub>, and CFS<sub>90</sub>/GFS<sub>90</sub>-based composites being superior to OPC and OPC-based concretes from the perspectives of economics (elemental sulfur and partially rancidified animal fats are low-value waste products), engineering (greater strength and resistance to damage mechanisms vs. OPC), and sustainability (replacing heavily CO<sub>2</sub>-emitting OPC with formally CO<sub>2</sub>-sequestering CFS<sub>90</sub> or GFS<sub>90</sub>), we envision CFS<sub>90</sub>, GFS<sub>90</sub>, and CFS<sub>90</sub>/GFS<sub>90</sub>-based composites serving as drop-in alternatives in a variety of construction, roadbuilding, and other structurally-demanding applications. The materials described herein are, therefore, being subjected to studies on their long-term (on the order of years) strength and geometry retention and related ASTM and ISO tests to assess their properties further compared to those of mineral products.

**Supplementary Materials:** The following supporting information can be downloaded at: <https://www.mdpi.com/article/10.3390/chemistry5040146/s1>: Figure S1. Stress–strain plots for measurements on the compression test cylinders for CFS<sub>90</sub>, CFS<sub>90</sub>-SF, and CFS<sub>90</sub>-GGBFS. Data in Table 1 are averages of three independent trials with errors reported as standard deviations; Figure S2. Stress–strain plots for measurements on the compression test cylinders for CFS<sub>90</sub>-MK and CFS<sub>90</sub>-FA. Data in Table 1 are averages of three independent trials with errors reported as standard deviations; Figure S3. Stress–strain plots for measurements on the compression test cylinders for CFS<sub>90</sub>, CFS<sub>90</sub>-SF, and CFS<sub>90</sub>-GGBFS after being submerged in 0.5 M H<sub>2</sub>SO<sub>4</sub> for 24 h. Data in Table 1 are averages of three independent trials with errors reported as standard deviations; Figure S4. Stress–strain plots for measurements on the compression test cylinders for CFS<sub>90</sub>-MK and CFS<sub>90</sub>-FA after being submerged in 0.5 M H<sub>2</sub>SO<sub>4</sub> for 24 h. Data in Table 1 are averages of three independent trials with errors reported

as standard deviations; Figure S5. Stress–strain plots for measurements on the compression test cylinders for GFS<sub>90</sub> and GFS<sub>90</sub>-GGBFS. Data in Table 1 are averages of three independent trials with errors reported as standard deviations; Figure S6. Stress–strain plots for measurements on the compression test cylinders for GFS<sub>90</sub>-MK and GFS<sub>90</sub>-SF. Data in Table 1 are averages of three independent trials with errors reported as standard deviations; Figure S7. Stress–strain plots for measurements on the compression test cylinders for GFS<sub>90</sub> and GFS<sub>90</sub>-GGBFS after being submerged in 0.5 M H<sub>2</sub>SO<sub>4</sub> for 24 h. Data in Table 1 are averages of three independent trials with errors reported as standard deviations; Figure S8. Stress–strain plots for measurements on the compression test cylinders for GFS<sub>90</sub>-MK and GFS<sub>90</sub>-SF after being submerged in 0.5 M H<sub>2</sub>SO<sub>4</sub> for 24 h. Data in Table 1 are averages of three independent trials with errors reported as standard deviations.

**Author Contributions:** Conceptualization, R.C.S.; methodology, R.C.S.; formal analysis, C.V.L.; investigation, C.V.L. (lead) and K.M.D. (supporting); resources, R.C.S.; data curation, C.V.L.; writing—original draft preparation, A.G.T., A.D.S. and R.C.S.; writing—review and editing, all authors; supervision, R.C.S.; funding acquisition, R.C.S. and A.D.S. All authors have read and agreed to the published version of the manuscript.

**Funding:** This research was funded by the National Science Foundation (US) grant number CHE-2203669 and a seed grant from the Animal Co-products Research and Education Center.

**Data Availability Statement:** Data not available in the manuscript or Supplementary Material may be requested from the corresponding author (rhett@clemson.edu).

**Conflicts of Interest:** The authors declare no conflict of interest.

## References

- Loiseau, E.; Saikku, L.; Antikainen, R.; Droste, N.; Hansjürgens, B.; Pitkänen, K.; Leskinen, P.; Kuikman, P.; Thomsen, M. Green economy and related concepts: An overview. *J. Clean. Prod.* **2016**, *139*, 361–371. [\[CrossRef\]](#)
- Merino-Saum, A.; Clement, J.; Wyss, R.; Baldi, M.G. Unpacking the Green Economy concept: A quantitative analysis of 140 definitions. *J. Clean. Prod.* **2020**, *242*, 118339. [\[CrossRef\]](#)
- Scrivener, K.L.; John, V.M.; Gartner, E.M. Eco-efficient cements: Potential economically viable solutions for a low-CO<sub>2</sub> cement-based materials industry. *Cem. Concr. Res.* **2018**, *114*, 2–26. [\[CrossRef\]](#)
- Gartner, E. Industrially interesting approaches to "low-CO<sub>2</sub>" cements. *Cem. Concr. Res.* **2004**, *34*, 1489–1498. [\[CrossRef\]](#)
- Turner, L.K.; Collins, F.G. Carbon dioxide equivalent (CO<sub>2</sub>-e) emissions: A comparison between geopolymer and OPC cement concrete. *Constr. Build. Mater.* **2013**, *43*, 125–130. [\[CrossRef\]](#)
- Khongprom, P.; Suwanmanee, U. Environmental benefits of the integrated alternative technologies of the portland cement production: Case study in Thailand. *Eng. J.* **2017**, *21*, 15–27. [\[CrossRef\]](#)
- Andrew, R.M. Global CO<sub>2</sub> emissions from cement production. *Earth Syst. Sci. Data* **2019**, *11*, 1675–1710. [\[CrossRef\]](#)
- Wolf, C.; Klein, D.; Weber-Blaschke, G.; Richter, K. Systematic review and meta-analysis of life cycle assessments for wood energy services. *J. Ind. Ecol.* **2016**, *20*, 743–763. [\[CrossRef\]](#)
- Rasmussen, F.N.; Andersen, C.E.; Wittchen, A.; Hansen, R.N.; Birgisdóttir, H. Environmental product declarations of structural wood: A review of impacts and potential pitfalls for practice. *Buildings* **2021**, *11*, 362. [\[CrossRef\]](#)
- Zhu, Y.; Romain, C.; Williams, C.K. Sustainable polymers from renewable resources. *Nature* **2016**, *540*, 354–362. [\[CrossRef\]](#)
- Fagnani, D.E.; Tami, J.L.; Copley, G.; Clemons, M.N.; Getzler, Y.D.Y.L.; McNeil, A.J. 100th Anniversary of Macromolecular Science Viewpoint: Redefining Sustainable Polymers. *ACS Macro Lett.* **2021**, *10*, 41–53. [\[CrossRef\]](#)
- Gowri, K. Green building rating systems: An overview. *ASHRAE J.* **2004**, *46*, 56.
- Tisdale, K.A.; Maladeniya, C.P.; Lopez, C.V.; Tennyson, A.G.; Smith, R.C. Sustainable Composites from Waste Sulfur, Terpenoids, and Pozzolan Cements. *J. Compos. Sci.* **2023**, *7*, 35. [\[CrossRef\]](#)
- Graham, M.J.; Lopez, C.V.; Maladeniya, C.P.; Tennyson, A.G.; Smith, R.C. Influence of pozzolans on plant oil-sulfur polymer cements: More sustainable and chemically-resistant alternatives to Portland cement. *J. Appl. Polym. Sci.* **2023**, *140*, e53684. [\[CrossRef\]](#)
- Smith, A.D.; Smith, R.C.; Tennyson, A.G. Polymer cements by copolymerization of waste sulfur, oleic acid, and pozzolan cements. *Sustain. Chem. Pharm.* **2020**, *16*, 100249. [\[CrossRef\]](#)
- Meyer, B. Solid allotropes of sulfur. *Chem. Rev.* **1964**, *64*, 429–451. [\[CrossRef\]](#)
- Meyer, B. The structures of elemental sulfur. *Adv. Inorg. Chem. Radiochem.* **1976**, *18*, 287–317.
- Kutney, G. *Sulfur: History, Technology, Applications & Industry*; ChemTec: Toronto, ON, Canada, 2007.
- Lim, J.; Pyun, J.; Char, K. Recent Approaches for the Direct Use of Elemental Sulfur in the Synthesis and Processing of Advanced Materials. *Angew. Chem. Int. Ed.* **2015**, *54*, 3249–3258. [\[CrossRef\]](#)
- U.S. Geological Survey. *Mineral Commodity Summaries 2017*; U.S. Geological Survey: Reston, VA, USA, 2017; p. 202. [\[CrossRef\]](#)

21. Worthington, M.J.H.; Kucera, R.L.; Chalker, J.M. Green chemistry and polymers made from sulfur. *Green Chem.* **2017**, *19*, 2748–2761. [[CrossRef](#)]
22. Crockett, M.P.; Evans, A.M.; Worthington, M.J.H.; Albuquerque, I.S.; Slattery, A.D.; Gibson, C.T.; Campbell, J.A.; Lewis, D.A.; Bernardes, G.J.L.; Chalker, J.M. Sulfur-Limonene Polysulfide: A Material Synthesized Entirely from Industrial By-Products and Its Use in Removing Toxic Metals from Water and Soil. *Angew. Chem. Int. Ed.* **2016**, *55*, 1714–1718. [[CrossRef](#)]
23. Bao, J.; Martin, K.P.; Cho, E.; Kang, K.-S.; Glass, R.S.; Coropceanu, V.; Bredas, J.-L.; Parker, W.O.N., Jr.; Njardarson, J.T.; Pyun, J. On the Mechanism of the Inverse Vulcanization of Elemental Sulfur: Structural Characterization of Poly(sulfur-random-(1,3-diisopropenylbenzene)). *J. Am. Chem. Soc.* **2023**, *145*, 12386–12397. [[CrossRef](#)]
24. Chung, W.J.; Griebel, J.J.; Kim, E.T.; Yoon, H.; Simmonds, A.G.; Ji, H.J.; Dirlam, P.T.; Glass, R.S.; Wie, J.J.; Nguyen, N.A.; et al. The use of elemental sulfur as an alternative feedstock for polymeric materials. *Nat. Chem.* **2013**, *5*, 518–524. [[CrossRef](#)]
25. Thiounn, T.; Lauer, M.K.; Bedford, M.S.; Smith, R.C.; Tennyson, A.G. Thermally-healable network solids of sulfur-crosslinked poly(4-allyloxystyrene). *RSC Adv.* **2018**, *8*, 39074–39082. [[CrossRef](#)] [[PubMed](#)]
26. Chen, Z.; Droste, J.; Zhai, G.; Zhu, J.; Yang, J.; Hansen, M.R.; Zhuang, X. Sulfur-anchored azulene as a cathode material for Li-S batteries. *Chem. Commun.* **2019**, *55*, 9047–9050. [[CrossRef](#)] [[PubMed](#)]
27. Zhao, F.; Li, Y.; Feng, W. Recent Advances in Applying Vulcanization/Inverse Vulcanization Methods to Achieve High-Performance Sulfur-Containing Polymer Cathode Materials for Li-S Batteries. *Small Methods* **2018**, *2*, 1–34. [[CrossRef](#)]
28. Nguyen, D.T.; Hoefling, A.; Yee, M.; Nguyen, G.T.H.; Theato, P.; Lee, Y.J.; Song, S.-W. Enabling High-Rate and Safe Lithium Ion-Sulfur Batteries by Effective Combination of Sulfur-Copolymer Cathode and Hard-Carbon Anode. *ChemSusChem* **2019**, *12*, 480–486. [[CrossRef](#)] [[PubMed](#)]
29. Mutlu, H.; Theato, P.; Ceper Ezgi, B.; Ozmen Mehmet, M.; Li, X.; Yang, J.; Dong, W.; Theato, P.; Yang, J. Sulfur Chemistry in Polymer and Materials Science. *Macromol. Rapid Commun.* **2019**, *40*, e1800650. [[CrossRef](#)]
30. Lopez, C.V.; Maladeniya, C.P.; Smith, R.C. Lithium-Sulfur Batteries: Advances and Trends. *Electrochem* **2020**, *1*, 226–259. [[CrossRef](#)]
31. Griebel, J.J.; Namnabat, S.; Kim, E.T.; Himmelhuber, R.; Moronta, D.H.; Chung, W.J.; Simmonds, A.G.; Kim, K.-J.; van der Laan, J.; Nguyen, N.A.; et al. New Infrared Transmitting Material via Inverse Vulcanization of Elemental Sulfur to Prepare High Refractive Index Polymers. *Adv. Mater.* **2014**, *26*, 3014–3018. [[CrossRef](#)] [[PubMed](#)]
32. Eder, M.L.; Call, C.B.; Jenkins, C.L. Utilizing Reclaimed Petroleum Waste to Synthesize Water-Soluble Polysulfides for Selective Heavy Metal Binding and Detection. *ACS Appl. Polym. Mater.* **2022**, *4*, 1110–1116. [[CrossRef](#)]
33. Lin, H.-K.; Lai, Y.-S.; Liu, Y.-L. Cross-Linkable and Self-Foaming Polysulfide Materials for Repairable and Mercury Capture Applications. *ACS Sustain. Chem. Eng.* **2019**, *7*, 4515–4522. [[CrossRef](#)]
34. Abraham, A.M.; Kumar, S.V.; Alhassan, S.M. Porous sulphur copolymer for gas-phase mercury removal and thermal insulation. *Chem. Eng. J.* **2018**, *332*, 1–7. [[CrossRef](#)]
35. Parker, D.J.; Jones, H.A.; Petcher, S.; Cervini, L.; Griffin, J.M.; Akhtar, R.; Hasell, T. Low cost and renewable sulfur-polymers by inverse vulcanization, and their potential for mercury capture. *J. Mater. Chem. A* **2017**, *5*, 11682–11692. [[CrossRef](#)]
36. Akay, S.; Kayan, B.; Kalderis, D.; Arslan, M.; Yagci, Y.; Kiskan, B. Poly(benzoxazine-co-sulfur): An efficient sorbent for mercury removal from aqueous solution. *J. Appl. Polym. Sci.* **2017**, *134*, 45306. [[CrossRef](#)]
37. Hasell, T.; Parker, D.J.; Jones, H.A.; McAllister, T.; Howdle, S.M. Porous inverse vulcanized polymers for mercury capture. *Chem. Commun.* **2016**, *52*, 5383–5386. [[CrossRef](#)] [[PubMed](#)]
38. Davis, A.E.; Sayer, K.B.; Jenkins, C.L. A comparison of adhesive polysulfides initiated by garlic essential oil and elemental sulfur to create recyclable adhesives. *Polym. Chem.* **2022**, *13*, 4634–4640. [[CrossRef](#)]
39. Herrera, C.; Ysinga, K.J.; Jenkins, C.L. Polysulfides Synthesized from Renewable Garlic Components and Repurposed Sulfur Form Environmentally Friendly Adhesives. *ACS Appl. Mater. Interfaces* **2019**, *11*, 35312–35318. [[CrossRef](#)]
40. do Valle, S.F.; Giroto, A.S.; Reis, H.P.G.; Guimarães, G.G.F.; Ribeiro, C. Synergy of Phosphate-Controlled Release and Sulfur Oxidation in Novel Polysulfide Composites for Sustainable Fertilization. *J. Agric. Food Chem.* **2021**, *69*, 2392–2402. [[CrossRef](#)]
41. Valle, S.F.; Giroto, A.S.; Klaic, R.; Guimaraes, G.G.F.; Ribeiro, C. Sulfur fertilizer based on inverse vulcanization process with soybean oil. *Polym. Degrad. Stab.* **2019**, *162*, 102–105. [[CrossRef](#)]
42. Mann, M.; Kruger, J.E.; Andari, F.; McErlean, J.; Gascooke, J.R.; Smith, J.A.; Worthington, M.J.H.; McKinley, C.C.C.; Campbell, J.A.; Lewis, D.A.; et al. Sulfur polymer composites as controlled-release fertilizers. *Org. Biomol. Chem.* **2019**, *17*, 1929–1936. [[CrossRef](#)]
43. Simmonds, A.G.; Griebel, J.J.; Park, J.; Kim, K.R.; Chung, W.J.; Oleshko, V.P.; Kim, J.; Kim, E.T.; Glass, R.S.; Soles, C.L.; et al. Inverse Vulcanization of Elemental Sulfur to Prepare Polymeric Electrode Materials for Li-S Batteries. *ACS Macro Lett.* **2014**, *3*, 229–232. [[CrossRef](#)] [[PubMed](#)]
44. Dirlam, P.T.; Simmonds, A.G.; Kleine, T.S.; Nguyen, N.A.; Anderson, L.E.; Klever, A.O.; Florian, A.; Costanzo, P.J.; Theato, P.; Mackay, M.E.; et al. Inverse vulcanization of elemental sulfur with 1,4-diphenylbutadiyne for cathode materials in Li-S batteries. *RSC Adv.* **2015**, *5*, 24718–24722. [[CrossRef](#)]
45. Griebel, J.J.; Li, G.; Glass, R.S.; Char, K.; Pyun, J. Kilogram scale inverse vulcanization of elemental sulfur to prepare high capacity polymer electrodes for Li-S batteries. *J. Polym. Sci. A* **2015**, *53*, 173–177. [[CrossRef](#)]
46. Arslan, M.; Kiskan, B.; Yagci, Y. Combining Elemental Sulfur with Polybenzoxazines via Inverse Vulcanization. *Macromolecules* **2016**, *49*, 767–773. [[CrossRef](#)]

47. Smith, A.D.; Smith, R.C.; Tennyson, A.G. Sulfur-Containing Polymers Prepared from Fatty Acid-Derived Monomers: Application of Atom-Economical Thiol-ene/Thiol-yne Click Reactions and Inverse Vulcanization Strategies. *Sustain. Chem.* **2020**, *1*, 209–237. [[CrossRef](#)]
48. Smith, A.D.; McMillin, C.D.; Smith, R.C.; Tennyson, A.G. Copolymers by Inverse Vulcanization of Sulfur with Pure or Technical Grade Unsaturated Fatty Acids. *J. Polym. Sci.* **2020**, *58*, 438–445. [[CrossRef](#)]
49. Lopez, C.V.; Karunarathna, M.S.; Lauer, M.K.; Maladeniya, C.P.; Thiounn, T.; Ackley, E.D.; Smith, R.C. High Strength, Acid-Resistant Composites from Canola, Sunflower, or Linseed Oils: Influence of Triglyceride Unsaturation on Material Properties. *J. Polym. Sci.* **2020**, *58*, 2259–2266. [[CrossRef](#)]
50. Hoefling, A.; Lee, Y.J.; Theato, P. Sulfur-Based Polymer Composites from Vegetable Oils and Elemental Sulfur: A Sustainable Active Material for Li-S Batteries. *Macromol. Chem. Phys.* **2017**, *218*, 1600303. [[CrossRef](#)]
51. Worthington, M.J.H.; Kucera, R.L.; Albuquerque, I.S.; Gibson, C.T.; Sibley, A.; Slattery, A.D.; Campbell, J.A.; Alboaiji, S.F.K.; Muller, K.A.; Young, J.; et al. Laying Waste to Mercury: Inexpensive Sorbents Made from Sulfur and Recycled Cooking Oils. *Chem. Eur. J.* **2017**, *23*, 16219–16230. [[CrossRef](#)]
52. Smith, J.A.; Green, S.J.; Petcher, S.; Parker, D.J.; Zhang, B.; Worthington, M.J.H.; Wu, X.; Kelly, C.A.; Baker, T.; Gibson, C.T.; et al. Crosslinker Copolymerization for Property Control in Inverse Vulcanization. *Chem. Eur. J.* **2019**, *25*, 10433–10440. [[CrossRef](#)]
53. Gupta, A.; Worthington, M.J.H.; Patel, H.D.; Johnston, M.R.; Puri, M.; Chalker, J.M. Reaction of sulfur and sustainable algae oil for polymer synthesis and enrichment of saturated triglycerides. *ACS Sustain. Chem. Eng.* **2022**, *10*, 9022–9028. [[CrossRef](#)]
54. Kolet, M.; Zerbib, D.; Nakonechny, F.; Nisnevitch, M. Production of Biodiesel from Brown Grease. *Catalysts* **2020**, *10*, 1189. [[CrossRef](#)]
55. Pastore, C.; Lopez, A.; Mascolo, G. Efficient conversion of brown grease produced by municipal wastewater treatment plant into biofuel using aluminium chloride hexahydrate under very mild conditions. *Bioresour. Technol.* **2014**, *155*, 91–97. [[CrossRef](#)] [[PubMed](#)]
56. Saucedo-Oloño, P.Y.; Borbon-Almada, A.C.; Gaxiola, M.; Smith, A.D.; Tennyson, A.G.; Smith, R.C. Thermal and Mechanical Properties of Recyclable Composites Prepared from Bio-Olefins and Industrial Waste. *J. Compos. Sci.* **2023**, *7*, 248. [[CrossRef](#)]
57. Lopez, C.V.; Smith, A.D.; Smith, R.C. High strength composites from low-value animal co-products and industrial waste sulfur. *RSC Adv.* **2022**, *12*, 1535–1542. [[CrossRef](#)]
58. Massazza, F. Pozzolanic cements. *Cem. Concr. Compos.* **1993**, *15*, 185–214. [[CrossRef](#)]
59. Mattes, R.D. Is there a fatty acid taste? *Annu. Rev. Nutr.* **2009**, *29*, 305–327. [[CrossRef](#)]
60. Mattes, R.D. Accumulating evidence supports a taste component for free fatty acids in humans. *Physiol. Behav.* **2011**, *104*, 624–631. [[CrossRef](#)]
61. Dave, D.; Ghaly, A.E. Meat spoilage mechanisms and preservation techniques: A critical review. *Am. J. Agric. Biol. Sci.* **2011**, *6*, 486–510.
62. Hoekstra, A.Y. The hidden water resource use behind meat and dairy. *Anim. Front.* **2012**, *2*, 3–8. [[CrossRef](#)]
63. Fritz, S.; See, L.; Carlson, T.; Haklay, M.; Oliver, J.L.; Fraisl, D.; Mondardini, R.; Brocklehurst, M.; Shanley, L.A.; Schade, S. Citizen science and the United Nations sustainable development goals. *Nat. Sustain.* **2019**, *2*, 922–930. [[CrossRef](#)]
64. Bleischwitz, R.; Spataru, C.; VanDeveer, S.D.; Obersteiner, M.; van der Voet, E.; Johnson, C.; Andrews-Speed, P.; Boersma, T.; Hoff, H.; Van Vuuren, D.P. Resource nexus perspectives towards the United Nations sustainable development goals. *Nat. Sustain.* **2018**, *1*, 737–743. [[CrossRef](#)]
65. Lopez, C.V.; Smith, A.D.; Smith, R.C. Evaluation of Animal Fats and Vegetable Oils as Comonomers in Polymer Composite Synthesis: Effects of Plant/Animal Sources and Comonomer Composition on Composite Properties. *Macromol. Chem. Phys.* **2023**, 2300233. [[CrossRef](#)]
66. Beauchamp, R.; Bus, J.S.; Popp, J.A.; Boreiko, C.J.; Andjelkovich, D.A.; Leber, P. A critical review of the literature on hydrogen sulfide toxicity. *CRC Crit. Rev. Toxicol.* **1984**, *13*, 25–97. [[CrossRef](#)]
67. Truong, D.H.; Eghbal, M.A.; Hindmarsh, W.; Roth, S.H.; O'Brien, P.J. Molecular mechanisms of hydrogen sulfide toxicity. *Drug Metab. Rev.* **2006**, *38*, 733–744. [[CrossRef](#)]
68. Ng, P.C.; Hendry-Hofer, T.B.; Witeof, A.E.; Brenner, M.; Mahon, S.B.; Boss, G.R.; Haouzi, P.; Bebart, V.S. Hydrogen sulfide toxicity: Mechanism of action, clinical presentation, and countermeasure development. *J. Med. Toxicol.* **2019**, *15*, 287–294. [[CrossRef](#)]
69. Alptekin, E.; Canakci, M. Optimization of pretreatment reaction for methyl ester production from chicken fat. *Fuel* **2010**, *89*, 4035–4039. [[CrossRef](#)]
70. Kirubakaran, M.; Selvan, V.A.M. A comprehensive review of low cost biodiesel production from waste chicken fat. *Renew. Sustain. Energy Rev.* **2018**, *82*, 390–401. [[CrossRef](#)]
71. Ahmaruzzaman, M. A review on the utilization of fly ash. *Prog. Energy Combust. Sci.* **2010**, *36*, 327–363. [[CrossRef](#)]
72. Siddique, R. Utilization of silica fume in concrete: Review of hardened properties. *Resour. Conserv. Recycl.* **2011**, *55*, 923–932. [[CrossRef](#)]
73. Özbay, E.; Erdemir, M.; Durmuş, H.İ. Utilization and efficiency of ground granulated blast furnace slag on concrete properties—A review. *Constr. Build. Mater.* **2016**, *105*, 423–434. [[CrossRef](#)]
74. Siddique, R.; Klaus, J. Influence of metakaolin on the properties of mortar and concrete: A review. *Appl. Clay Sci.* **2009**, *43*, 392–400. [[CrossRef](#)]

75. Lauer, M.K.; Estrada-Mendoza, T.A.; McMillen, C.D.; Chumanov, G.; Tennyson, A.G.; Smith, R.C. Durable Cellulose-Sulfur Composites Derived from Agricultural and Petrochemical Waste. *Adv. Sustain. Syst.* **2019**, *3*, 1900062. [[CrossRef](#)]
76. Yan, P.; Zhao, W.; Tonkin, S.J.; Chalker, J.M.; Schiller, T.L.; Hasell, T. Stretchable and Durable Inverse Vulcanized Polymers with Chemical and Thermal Recycling. *Chem. Mater.* **2022**, *34*, 1167–1178. [[CrossRef](#)]
77. Yan, P.; Zhao, W.; Zhang, B.; Jiang, L.; Petcher, S.; Smith, J.A.; Parker, D.J.; Cooper, A.I.; Lei, J.; Hasell, T. Inverse vulcanized polymers with shape memory, enhanced mechanical properties, and vitrimer behavior. *Angew. Chem. Int. Ed.* **2020**, *59*, 13371–13378. [[CrossRef](#)]
78. Hanna, V.; Yan, P.; Petcher, S.; Hasell, T. Incorporation of fillers to modify the mechanical performance of inverse vulcanised polymers. *Polym. Chem.* **2022**, *13*, 3930–3937. [[CrossRef](#)]

**Disclaimer/Publisher's Note:** The statements, opinions and data contained in all publications are solely those of the individual author(s) and contributor(s) and not of MDPI and/or the editor(s). MDPI and/or the editor(s) disclaim responsibility for any injury to people or property resulting from any ideas, methods, instructions or products referred to in the content.